Journal of Structural Geology 32 (2010) 107–117

Contents lists available at ScienceDirect

Journal of Structural Geology

journal homepage: www.elsevier.com/locate/jsg

Magnitude of weakening during crustal-scale shear zone development

Christopher Gerbi [a,*], Nicholas Culshaw [b,1], Jeffrey Marsh [a,2]

[a] Department of Earth Sciences, University of Maine, Orono, ME 04469, United States
[b] Department of Earth Sciences, Dalhousie University, Halifax B3H 3J5, Canada

ARTICLE INFO

Article history:
Received 17 January 2009
Received in revised form
4 September 2009
Accepted 5 October 2009
Available online 13 October 2009

Keywords:
Shear zone
Strain weakening
Grenville Province
Rheology

ABSTRACT

We describe and apply a field-based approach for calculating the bulk strength of a heterogeneous material to a crustal-scale shear zone defining the margin of the Ma Parry Sound domain in the Grenville Province of southeastern Ontario. Using a numerical method, we calculate bulk strength, defined as effective viscosity, as the ratio between the surface traction needed to deform a square block in simple shear and the velocity gradient across that block. We use natural shear zone geometries to define the internal block structure and assign internal relative viscosities based primarily on textural criteria. The margin of the Parry Sound domain developed into the km-scale Twelve Mile Bay shear zone, accommodating several tens of km of transport, while the domain interior remained rigid. Fracturing and fluid infiltration drove development of an amphibolite facies meter-scale shear zone network that evolved into the Twelve Mile Bay structure. We analyzed three sites across the ~5 km-wide strain gradient from near the granulitic domain to the large scale shear zone. The rocks at the shear zone margin weakened by approximately 30%. Those in the core weakened by at least 77% and probably by an order of magnitude. These values lie between but differ substantively from the isostress and isostrain-rate bounds, indicating that a numerical approach such as presented here markedly improves the accuracy of bulk strength calculations.

1. Introduction

Spatial and temporal strength variation throughout the crust influences geodynamic processes as disparate as orogenic topographic evolution (e.g., Dahlen et al., 1984; Beaumont et al., 2001; Groome et al., 2008) and post-glacial rebound (Larsen et al., 2005; Wu and Mazzotti, 2007). In addition, and more directly, strength variation affects or controls the strain distribution in a region. Our understanding of crustal strength derives in large part from three sources: experimental deformation, geodesy, and numerical and analogue modeling. From these sources, some general pictures of crustal strength emerge (e.g., Kohlstedt et al., 1995; Handy et al., 2007; Bürgmann and Dresen, 2008), but considerable uncertainty remains about the rheological structure in natural orogens (cf., for example, Jackson, 2002; Handy and Brun, 2004). Complicating a general description of rheological structure, processes such as metamorphism, melting and magma migration, fluid infiltration, and deformation all operate during orogenesis. Experimental and theoretical studies can constrain the rheological effects of some of these processes, but thorough understanding requires field-based investigation of synorogenic strength changes. In this contribution, we employ a numerical method for calculating bulk strength based on natural structures, documenting an effective viscosity drop of approximately an order of magnitude at the margins of a granulitic domain where it developed into an upper amphibolite facies km-scale shear zone. Interpretations of spatial strength variation exist (e.g., Houseman et al., 2008), but we are not aware of any field-based study documenting the temporal strength change associated with the development of a shear zone network.

2. Background

2.1. Controls on and calculations of rock strength

Rock strength follows many definitions depending on the material type (e.g., viscous, plastic, elastic, and combinations thereof). We frame this study around mechanics in the middle and lower orogenic crust, well below the frictional–viscous transition, so we define strength as effective viscosity: the instantaneous ratio between stress and strain rate. The dominant factors controlling the bulk effective viscosity of a rock include mineralogy, phase or unit geometry (e.g., Handy, 1990, 1994; Ji, 2004; Takeda and Griera,

* Corresponding author. Tel.: +1 207 581 2153; fax: +1 207 581 2022.
E-mail addresses: gerbi@umit.maine.edu (C. Gerbi), culshaw@dal.ca (N. Culshaw), jeff_marsh@umit.maine.edu (J. Marsh).
[1] Tel.: +1 902 494 3501.
[2] Tel.: +1 207 581 2221.

0191-8141/$ – see front matter © 2009 Elsevier Ltd. All rights reserved.
doi:10.1016/j.jsg.2009.10.002

2006), fluid and/or melt content (e.g., Holl et al., 1997; Brown and Solar, 2000; Evans, 2005; Rosenberg and Handy, 2005), and temperature. In general, weaker minerals, a higher degree of weak-phase interconnectivity, higher fluid or melt content, and higher temperatures reduce strength.

The strength of polyphase materials lies between the isostress (Reuss, 1929) and isostrain-rate (Voigt, 1928) bounds (e.g., Handy, 1990, 1994; Handy et al., 1999; Tullis et al., 1991; Bons and Urai, 1994; Ji, 2004). The former describes a state in which all phases experience the same stress, usually associated with strong inclusions in a softer matrix. The latter describes a state in which all phases deform at the same rate, usually associated with soft inclusions in a stronger matrix. Handy (1990) described two characteristic microstructures for ductilely deforming polyphase rocks: a load-bearing framework and interconnected weak layers. The latter is markedly weaker, lying close to the isostress bound, and can be stable at high strain. A load-bearing framework is stronger, lying near the isostrain-rate bound, but generally unstable and can evolve into the geometrically more stable interconnected weak layer geometry either mechanically (Handy, 1994; Lonka et al., 1998; Handy et al., 1999), or with the presence of even a small percentage of melt (Rosenberg and Handy, 2005). Calculation of the theoretical isostress and isostrain-rate bounds simply requires knowledge of the strengths of the individual phases and their volume fraction; these bounding definitions take no explicit account of the phase distribution. But because the phase distribution controls where between the strength bounds the bulk strength lies, it is a fundamental determinant of rock strength. Ji (2004) modified the isostress and isostrain-rate formulations to include a parameter, *J*, to account for the phase geometry. Similarly, Bons and Urai (1994) suggested that the distance between the bounds is proportionally constant, relative to volume fraction, for a given microstructure that they defined as related to the percolation threshold. Unfortunately, no robust *a priori* method exists to derive either *J* or the percolation threshold for complex natural structures, limiting the value of those approximations. Treagus (2002) calculated the bulk viscosity of two-phase mixtures with various idealized geometries based on conglomerates and concluded that both volume fraction and shape fabric are critical controls on the aggregate strength. Her results, however, which are based on an inclusion-matrix structure, do not directly apply to more general structural geometries in naturally deformed rocks. Tullis et al. (1991) developed a numerical approach to calculate bulk flow properties based on digitizing the phase or unit distribution and providing a flow law for each component. Their approach works well if the individual flow laws are well-characterized, but it is also a time-consuming methodology. To date, analytical approaches to calculating bulk rock strength are too imprecise for most situations, which therefore require a numerical approach such as used by Tullis et al. (1991) or the one described below. Both numerical and analytical approaches require knowing the individual phase properties accurately.

2.2. Magnitude of weakening

Rocks can weaken either uniformly or through the development of localized high strain zones. Both mechanisms can develop for similar reasons, but local feedback and rate relationships influence which dominates at which scale. In the upper crust, faults appear to be up to five to ten times weaker than their host rocks (Zoback, 2000). Rutter (1999) has postulated up to a 50% decrease in strength at the regional scale due to shear zone development. Parallel to the factors that control rock strength, the dominant factors that affect the degree of strength change include metamorphic reactions (e.g., Rubie, 1983; Wintsch et al., 1995; Groome et al., 2006; Upton and Craw, 2008), structural or textural evolution (e.g., Handy, 1994; Johnson et al., 2004), fluid flux, melting, and temperature changes. Of these factors, melting induces the greatest strength change, as melt viscosities may be up to 14 orders of magnitude lower than their solid counterparts (Cruden, 1990; Pinkerton and Stevenson, 1992). During most tectonism, the strength drop is significantly less, as the deforming rocks would likely host only a small melt percentage, but still could be more than an order of magnitude (Rosenberg and Handy, 2005).

Using the strengths of the constituent phases in addition to analytical flow laws generated for polyphase materials and mylonites (e.g., Jordan, 1987; Hueckel et al., 1994; Handy, 1994; Handy et al., 1999; Treagus, 2002; Ji et al., 2004), some studies estimate the strength change during shear zone formation, but with little direct application to natural systems. For example, based on the analytical equations of Handy et al. (1999), an analysis by Park et al. (2006) implies strength drops of approximately 25% and 70% for nonmica- and mica-bearing weak layers, respectively. Modeling viscoelastic deformation of strong- and weak-phase interconnected geometries, Takeda and Griera (2006) track changes in bulk effective viscosity in a shearing model block. They calculate little weakening in models in which the initial structure includes an interconnected weak layer. Weakening up to 50% occurs as a strong-phase-supporting framework evolves towards highly elongate weak layers.

Experimental studies provide more robust quantitative data but trade that improvement for greater extrapolations to natural conditions and larger scales and therefore greater uncertainty under those conditions. Experiments investigating strain weakening (e.g., Jordan, 1987; Dell'Angelo and Tullis, 1996; Ross and Wilks, 1996; Rybacki et al., 2003; Dimanov and Dresen, 2005; Bystricky et al., 2006; Holyoke and Tullis, 2006) have produced a range of results. For example, deformation of an orthopyroxene granulite (Ross and Wilks, 1996) and an aplite (Dell'Angelo and Tullis, 1996) yielded a range of 15–50% weakening between the original material and the development of quasi-steady-state flow. To evaluate the role of developing an interconnected weak layer from a load-bearing framework, Holyoke and Tullis (2006) deformed a quartzofeldspathic gneiss and observed strength drops of 30–60%. The degree of strength drop varied with temperature and strain rate.

2.3. Geologic setting

The southwestern Canadian Grenville Province (Fig. 1), along the shores of Georgian Bay in Lake Huron, represents the deeply eroded (to depths equivalent to ~1.0–1.3 GPa) roots of an orogenic belt with a size and tectonometamorphic history comparable to the modern Himalayan orogen. In the Georgian Bay region, km-scale shear zones separate lithotectonic domains within the allochthonous portion of the orogen (Culshaw et al., 1997, 2004). The Grenville orogen formed between approximately 1190 Ma and 980 Ma (Rivers, 1997) and consists of a complex arrangement of tectonic blocks along its several thousand kilometers of length. The Parry Sound domain, which lies within the Central Gneiss Belt of Ontario, comprises metasediments, arc-related mafic through felsic orthogneisses, and anorthosite originally formed ca. 1400–1160 Ma (Culshaw et al., 1997). Internal assembly of the tectonic stratigraphy in the Parry Sound domain and associated granulite facies metamorphism occurred ca. 1160 Ma (van Breeman et al., 1986; Wodicka et al., 2000). The Parry Sound domain as a whole is an allochthonous nappe and was emplaced along the kms-wide Twelve Mile Bay shear zone (Davidson et al., 1982; Davidson, 1984; Culshaw et al., 1997) in probably two stages, with the second stage as late as 1050 Ma (Krogh and Kwok, 2005).

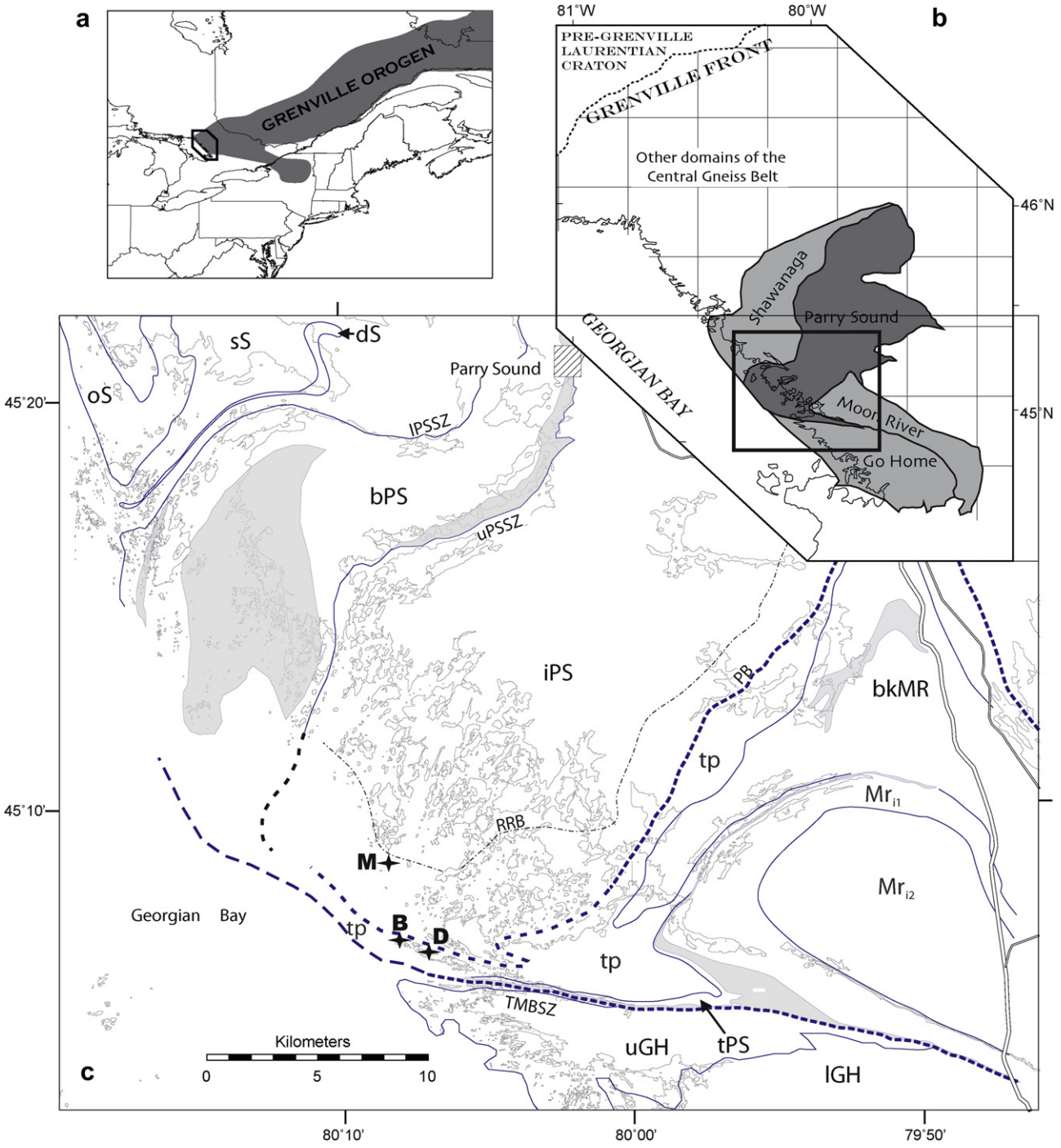

Fig. 1. Geology of study area. (a) The Grenville orogen in eastern North America. Box marks B. (b) Domains of the Central Gneiss Belt germane to this study. Box marks C. (c) Geologic map of the southwestern Parry Sound domain and adjacent domains. After Culshaw and Gerbi (2009). M, D, B – Matches, Dogleg, and Boomerang Islands. Shawanaga domain: oS, sS, dS – Ojibway and Sand Bay gneiss associations, Dillion schist. Parry Sound domain: bPS, iPS, tPS, tp – basal, interior Parry Sound domains, Twelve Mile Bay assemblage, and transposed gneiss derived from Parry sound domain (Culshaw and Gerbi, 2009). Moon River domain: bKMR, MRi1-i2 – Blackstone gneiss association, interior subdivisions of Moon River domain. Go Home domain: uGH, lGH – upper, lower divisions. lPSSZ – lithological boundary within lower strand of Parry Sound shear zone. uPSSZ – lithological boundary at upper margin of upper strand of Pasrry Sound shear zone. TMBSZ – Twelve Mile Bay shear zone. PB – inboard margin of transposed gneiss. RRB – boundary of substantial retrogression in Parry Sound domain. Gray shaded areas represent anorthosite.

This emplacement caused the development of widespread outcrop-scale shear zones along the domain margins. The shear zones developed in conjunction with a retrograde transition from granulite to upper amphibolite facies assemblages (Wodicka et al., 2000; Culshaw et al., 2004; Culshaw and Gerbi, 2009). The transformation progresses from relict granulite facies textures and mineralogy in the center of the domain to fully transposed gneiss of the Twelve Mile Bay shear zone at the contact with the underlying Go Home domain. The progressive weakening occurs in the following sequence (Fig. 2): (1) Due to high fluid pressure, the granulite facies orthogneisses developed fractures, which filled with pegmatites and fluids. (2) Fluids derived from the fractures

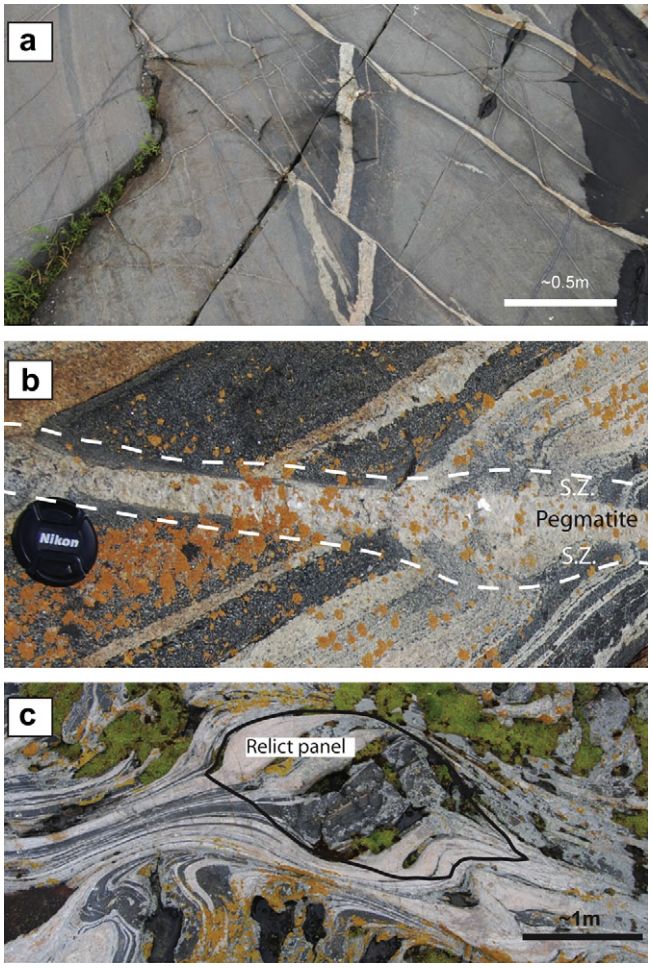

Fig. 2. Stages of development of the transposed fabric associated with the Twelve Mile Bay shear zone. (a) Fractures, most in a rectilinear pattern, fill with pegmatites and hydrate fracture walls. (b) Hydrated, weaker rock adjacent to pegmatite begins to shear ("s.z."). (c) Shear zones widen and coalesce, isolating blocks of undeformed or weakly deformed protolith ("relict panel").

infiltrated the host rock, weakening it through both the presence of fluids and metasomatic reactions. (3) Shear zones nucleated on the weak planes, eventually coalescing into networks around relict granulitic panels. (4) Closer to the domain boundary, shear zones widened and increasingly linked; in some locations transposition and retrogression are complete, with no granulite relicts remaining. This sequence suggests that strain localization along the boundary of the Parry Sound domain was caused by syntectonic weakening driven first by fluid infiltration then by textural development through shear zone linking. The exact processes of localization (cf. Carreras, 2001; Montesi and Zuber, 2002; Jessell et al., 2009) are under active investigation, but do not affect the results of this work, as our calculations rely on the final deformation state rather than its temporal development.

3. Strength calculations

3.1. Method

For the purposes of this study, we want to document the change in decameter-scale bulk strength across a kilometers-long gradient. Although the methods are scale-independent, we focus on features mappable in the field. Our calculations follow two steps: first, map the natural geometry; second, perform a numerical calculation to determine bulk strength. As justified below, we assume simple shear, which allows us to use the following relationship:

$$\tau_{xy} = \eta \frac{\partial U_x}{\partial y} \tag{1}$$

where τ is shear stress, η is bulk effective viscosity, U is velocity and x and y define the orthogonal spatial reference frame. Mapping criteria depend on the system under study. For this project, we defined two units: relict granulite and transposed fabric.

All calculations of bulk effective viscosity presented here are based on the numerical deformation of a two-dimensional square using a dimensionless finite element method (Fig. 3). Elle, a publicly available microdynamics code (Bons et al., 2008), transforms a pixel-based structure or microstructure, including the phase viscosities, to a form usable by Basil, a dimensionless viscous deformation code (Barr and Houseman, 1996; Houseman et al., 2008). The horizontal and vertical boundaries are of unit length. In keeping with the dimensionless nature of the calculations, rather than prescribe absolute viscosities, we use relative viscosities, whose values we obtain by the method described below. Based on a coordinate origin at the lower left corner of the model block, we deform the initial square in simple shear for one time step at a dimensionless velocity of -0.5 along $y = 1$ and 0.5 along $y = 0$, producing a sinistral shear sense (Fig. 3). Because we seek the effective viscosity for the given natural structures, we run for only a single time step and do not investigate texture evolution. Using Equation (1) and realizing that the modeled velocity gradient is unity, effective viscosity becomes numerically equivalent to the upper and lower boundary shear traction, τ_{xy}, required to generate the prescribed strain rate. We assume that homogeneous deformation sufficiently approximates the bulk behavior of the system, and tests indicate that this is an appropriate approximation for the geometries used here. For perfectly homogeneous deformation, the traction along the top and bottom boundaries would be equal; in our model runs, they differ up to a few percent. In the calculations, we use the average of the traction along the upper and lower boundaries.

We make two approximations, neither of which substantively affects the results. First, we approximate the strain as simple shear

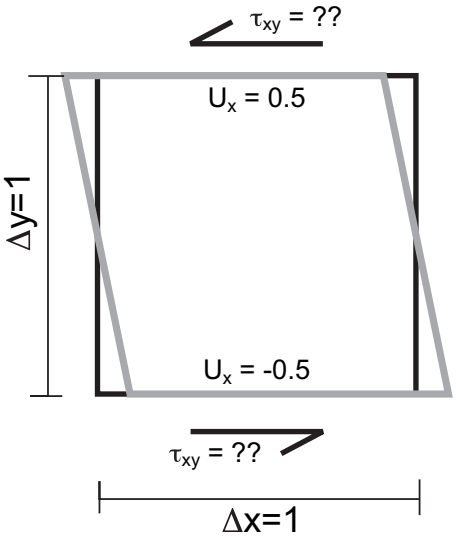

Fig. 3. Geometrical representation of dimensionless bulk effective viscosity calculation method. Black square represents the starting geometry. We map the natural shear zone network geometry, with viscosity variations, onto the square, which we then shear at a prescribed velocity gradient. Model output includes the traction needed to perform the deformation. We then calculate the bulk viscosity using Eq. (1).

perpendicular to view direction. Doubtless, some degree of strain out of the mapped plan exists, but the block geometry and hinge lines at the shear zone margins normal to the inferred transport direction suggest that simple shear dominated. If a small component of pure shear exists, our calculations would represent a minimum strength. Second, the numerical calculations are predicated on the approximation that we can identify an effective viscosity structure for a given point in time. A corollary approximation is that all fabric mapped as transposed, or "new", exhibited the same viscosity and was simultaneously active. Jessell et al. (2005, 2009), among others, have shown that this is not strictly true in many cases and that sites of localization vary during deformation. If parts of the mapped shear zone network were inactive, our calculations again represent a minimum strength. Nevertheless, we assert that this approximation does not substantially affect the results for the following reasons: (1) because all shear zones in an area appear to exhibit the same textures and mineral assemblages, inactive shear zones would still be substantially weaker than the relict panels, (2) we do not find evidence for cross-cutting relationships between shear zones, implying that all shear activity was broadly coeval, and (3) calculated results are not sensitive to small changes in the areal proportion of shear zones. In addition, the very high strain gradients at the margin of the shear zones (e.g., Fig. 2) justify using a two-phase mixture, shear zones and panels, rather than a more complicated geometry that would differentiate shear zone cores from flanks.

3.2. Estimating viscosity contrast

Several methods exist for estimating relative viscosities at the outcrop scale, including foliation refraction (Treagus, 1999) and boudinage geometry (Treagus and Lan, 2003, 2004). In addition, for a polyphase material comprising two materials of different strengths wherein the strong phase is isolated, we can expect that the strain ratio between the two materials will be the same as the viscosity contrast because the stress field is approximately uniform in such a geometry (e.g., Handy, 1994). If materials with different strengths experience the same stress for the same duration, they will deform at to a degree proportional to the strength contrast. However, due to the difficulty quantifying strain and the lack of boudinage and foliation refraction, we cannot apply these methods to most of the Parry Sound rocks. We therefore base our determination of viscosity contrast on a more qualitative approach. Numerical models (Fig. 4 and see also Jessell et al., 2009) illustrate that effective viscosity contrasts of greater than an order of magnitude yield negligible strain in the hard phase or unit. Although the degree of phase strain depends on the bulk strain, for places where "high" strain zones (e.g., Fig. 5a) surround un- to weakly deformed panels, we can infer viscosity contrasts of at least an order of magnitude. More than two orders of magnitude difference renders a panel effectively rigid. Greater deformation (Fig. 5b) in the panels yields lower viscosity contrasts, assigned on a case-by-case basis.

Deformation in the shear zones was accommodated largely by dislocation creep, implying that the rock behaves as a power-law material. Although modeling in Elle and Basil is possible (Houseman et al., 2008; Jessell et al., 2009), we choose to restrict ourselves to the effective viscosity because (1) we are not investigating any time-dependent behavior so effective viscosity is an appropriate representation of strength contrast, (3) use of a power-law formulation would introduce additional uncertainty because the flow law parameters are not well known; we can only infer relative contrasts from the field geometries, and (3) due to the hydration inducing the weakening, the flow laws for the panels and shear zones would differ, requiring us to develop multiple flow laws, again introducing greater uncertainty. Jessell et al. (2009) acknowledge the challenge in using localization geometry to infer paleo-rheology, as non-linear and linear viscous materials with appropriate parameters can produce similar results. The approach presented here does not speak to linear vs. non-linear behavior, but rather allows access to different paleo-rheological information.

3.3. Site results

We have quantified weakening at three sites associated with the Twelve Mile Bay shear zone (Fig. 1). The first site, Matches Island, represents the initial stages of shear zone development, and two unnamed islands, informally referred to here as Dogleg and Boomerang Islands, represent the edge of the shear zone core.

3.3.1. Matches Island

This islet (Fig. 6a) lies near the margin of the extension of the Twelve Mile Bay shear zone within the unretrogressed granulitic core of the Parry Sound domain and consists of two lithologic units: Unit 1 is a meter-scale layered mafic and felsic orthogneiss, and Unit 2 is an intermediate gneiss with pink granitic layers. Unit 2 retains no field evidence of its granulitic heritage and comprises an amphibolite facies plagioclase–quartz–hornblende–biotite assemblage. Because strain in Unit 2 did not manifest itself in discrete shear zones, but rather appears to have deformed more homogeneously, Unit 2 is not appropriate for the calculations presented here. We therefore concentrate on Unit 1, which is the dominant lithology in the area surrounding Matches Island. Unit 1 contains relict granulite textures and mineralogy in the undeformed panels between the shear zones. In places in the mafic panels, hornblende and biotite exhibit reaction textures around pyroxene, but original plagioclase–orthopyroxene–clinopyroxene patches persist throughout. The granitic layers contain plagioclase–alkali feldspar–quartz–hornblende–biotite assemblages in both the panels and shear zones. The

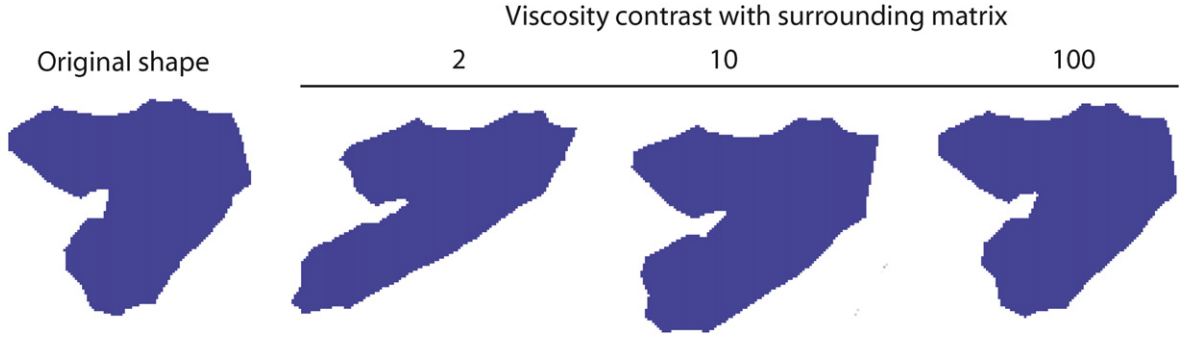

Fig. 4. Comparison of shape changes with viscosity contrast. We deformed the original shape under dextral simple shear using Elle and Basil software packages for three different viscosity contrasts between the shape and the surrounding matrix. Deformation of the object necessarily depends on bulk finite strain, but the comparisons among the different strength objects for the same finite strain yield a qualitative framework for estimating viscosity contrast. For contrasts greater than 10, deformation of the strong object is minimal.

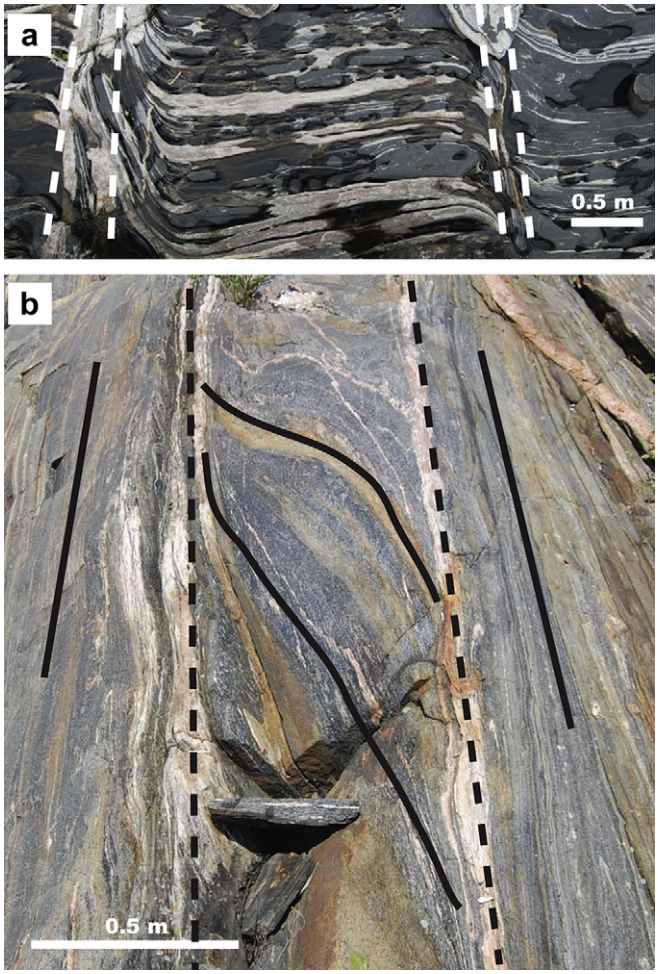

Fig. 5. Examples of panel types. (a) Undeformed panels separated by shear zones normal to granulitic layering on Matches Island. Dotted lines demarcate shear zones. (b) Sheared panel (within dashed lines) between zones of fully transposed gneiss on Dogleg Island. Solid lines are foliation form lines.

shear zones, nearly all of which are dextral, in the north and west portions of Unit 1 trend northwest–southeast and are poorly connected. Trends swing anticlockwise towards the east and increase in number and connectivity in the center of the island.

In order to base our calculations on a representative geometry, we selected an area within Unit 1 that includes both strongly and weakly interconnected regions. We constructed the viscosity, or shear zone, geometry (Fig. 7a) from a dGPS map constructed normal to the transport direction. In the model map, shear zones cover 19% of the area of Unit 1. To cover the range of possible variation, we calculated the bulk effective viscosity using viscosity contrasts of 2, 5, 10, and 50 between the shear zones and panels (Table 1).

Results (Fig. 8a) over that viscosity contrast range indicate strength drops from 11% to 48% relative to the panel strength. Here, we take panel strength as the original strength of the unit, given that relict granulite textures, including lineations, and assemblages persist and that there is no evidence of amphibolite facies deformation within the panels that would suggest that the panels somehow weakened prior to or synchronously with shear zone network development. For all viscosity contrasts, the calculated bulk weakening lies approximately halfway between the isostress and isostrain-rate bounds, with the actual position varying with viscosity contrast.

To more accurately determine the degree of weakening of the system, we must better constrain the viscosity contrast between panels and shear zones. The lack of deformation in the panels adjacent to shear zones with shear strains as high as 20 (calculated using dGPS measurements and the a–a' method of Ramsay and Huber, 1987) suggest that the panels were effectively rigid relative to the shear zones. Therefore, as a conservative choice, we base further discussion on a viscosity contrast of 10, chosen as a point at which little deformation occurs in the strong material (e.g., Jessell et al., 2009) and therefore a bulk weakening of 31% relative to the original rock (Table 1). The shear zones could reasonably have been more than an order of magnitude weaker than the panels, so we consider a bulk weakening of 30% as a minimum for this site. To determine how representative the selected area is, we also performed calculations for a subset of the selected area and an area further north on the island. Results from those calculations indicate that some heterogeneity exists but is relatively minor.

3.3.2. Dogleg and Boomerang Islands

These two islets lie in comparable structural positions north of the Twelve Mile Bay shear zone core, but well within the high strain portion. Both consist of wider shear zones and higher proportions of transposed gneiss than at Matches Island (Fig. 6b,c). Nevertheless, many panels preserve granulite textures. Transposed zones are more linked that at Matches Island, with relict panels generally more lozenge-shaped and less rectilinear. Some cm-scale shear zones cut across panels. The granulitic protolith was not identical to that on Matches Island in that the meter-scale layering was absent, but the lithologies are generally similar. Margins of the panels exhibit high strain gradients, similar to those on Matches Island. Units on the islands are easily divisible into transposed and untransposed gneiss. Because the features are larger than on Matches, we mapped representative areas and geometries using aerial photographs whose plane contained the transport direction and was perpendicular to layering.

Because of their similar structural position and the similar bulk strengths, we consider Boomerang and Dogleg Islands together. Shear zone areas for Dogleg and Boomerang Islands are 33% and 43%, respectively. This difference in coverage combined with the different shear zone geometry (Fig. 7b,c) yields similar strength changes (Table 1): for viscosity contrasts of 2, 5, 10, and 50, the bulk weakening averages to 25%, 54%, 70%, and 90% relative to the panels at those sites (Fig. 8). The proportional distance of the calculated strength between the isostress and isostrain-rate bounds changes markedly with viscosity contrast and varies between islands (Table 2). Although their bulk strengths are similar, the proportional difference between the bounds varies from 40% to 14% for Boomerang Island and 22% to 8% for Dogleg Island.

We have no definitive strain markers to aid in determining the appropriate panel-shear zone viscosity contrast. Given that in many locations we cannot trace units across the meter-scale shear zones, we posit shear strains greater than 10, in accordance with estimates from Matches Island. Shear strain within deformed panels, measured using the shear angle and assuming original orthogonality between panel and shear zone (cf. Twiss and Moores, 1992), is in general less than 2 (e.g., Fig. 5b). Thus, deformation observed in the panels is consistent with that of a viscosity contrast with the shear zones of no more than 10, and probably closer to 5. Our preferred estimate of bulk weakening relative to panel strength is therefore approximately 50%.

For a more rigorous treatment of Boomerang Island we assigned a greater viscosity to panels in the southern half of the island, as suggested by generally greater preservation of granulite textures and more rectilinear panels there. With a viscosity contrast of 10 for the southern panels and 5 for the northern panels, the bulk weakening was nearly identical to that on Dogleg Island calculated using a viscosity contrast of 5. The variation in panel strain on Boomerang Island, where the stronger panels resemble those on Matches Island, suggests that deformed panels both there and at Dogleg Island were

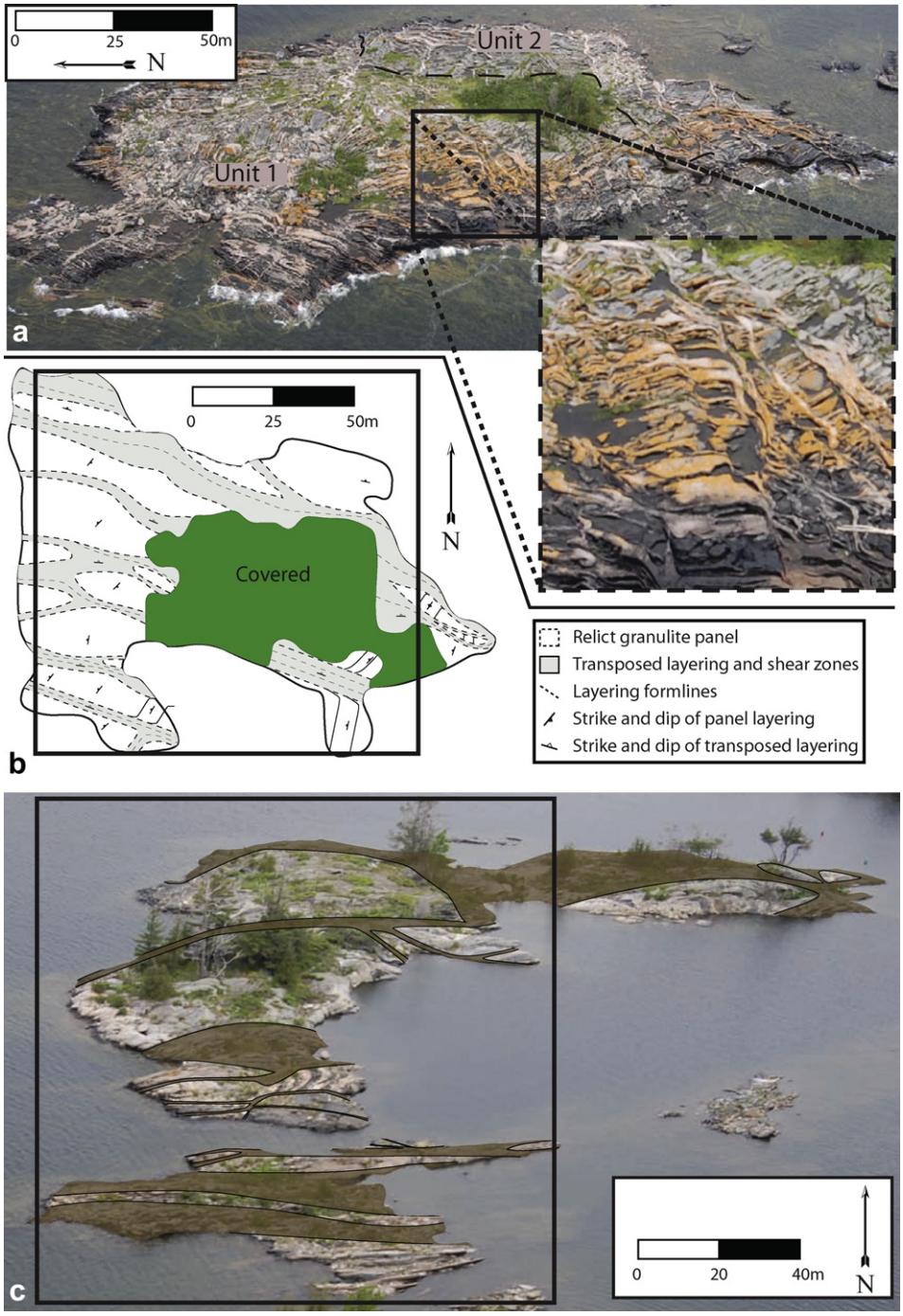

Fig. 6. Islands analyzed for bulk weakening. See Fig. 7 for viscosity maps, whose coverages are marked by boxes. We mapped through the water or extrapolated shear zones where viscosity maps do not coincide with land. (a) Matches Island. (b) Boomerang Island; light gray delineates shear zones. (c) Dogleg Island; dark areas are shear zones.

weaker than those on Matches Island. Yet until we quantify the relative strengths of the deformed panels to those on Matches Island, we cannot compare the results and produce an estimate for weakening across the full Twelve Mile Bay shear zone structure.

3.4. Transect results

The magnitude of weakening due to structural and metamorphic evolution at a specific site can be valuable information, and in the case of Matches Island, we have documented how at least a portion of that structure weakened by at least 30%. For the purposes of this contribution, however, we are concerned with the weakening into the domain-bounding Twelve Mile Bay shear zone. The site analysis presented above for Dogleg and Boomerang Islands cannot have regional relevance without identifying the relationship between the panel strength during shear zone formation and the original, granulite panel strength.

Structural and petrological evidence strongly suggests that the rocks of the Twelve Mile Bay shear zone derived from the Parry Sound interior. As discussed above, many of the panels near the Twelve Mile Bay shear zone deformed moderately but did not approach full transposition, whereas the panels at Matches remained rigid. Thus, the overall strength drop from the granulitic Parry Sound domain rocks is larger than that calculated for Dogleg or Boomerang Islands

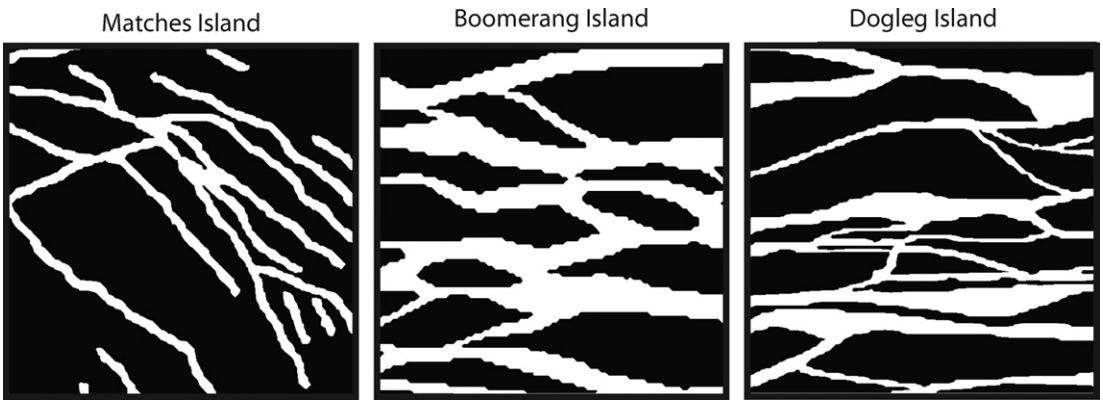

Fig. 7. Viscosity maps of the three study sites, illustrating the pattern of weak and strong zones used in the calculation of bulk strength. We varied the viscosities to test the sensitivity of the results to the viscosity contrast (see Table 1 for values used). White represents the lower viscosity shear zones; black, the higher viscosity panels. Stepped, rather than smooth, boundaries are due to model digitization.

alone. If we assign a somewhat conservative average factor of two strength difference between Matches Island panels (i.e., original granulite) and those within the margins of the Twelve Mile Bay shear zone, then the bulk strength drop between the granulitic protolith (i.e., panels at Matches Island) and the Twelve Mile Bay shear zone margins approaches an order of magnitude, at 77% (Table 3). In the core of the Twelve Mile Bay shear zone, more of the gneiss is transposed and fewer panels are undeformed, so this strength drop represents a minimum value for the viscosity factors used.

Alternatively, we could make a simple, first-order assumption that the shear zones preserved on Matches Island are the same strength as the transposed gneiss of the Twelve Mile Bay shear zone core. As the panels on Matches Island are essentially undeformed, we could therefore assert that the Twelve Mile Bay shear zone is at least an order of magnitude weaker than its granulitic protolith. This interpretation is consistent with our site-specific calculations, implying that the outcrop-scale shear zones were indeed of comparable strength across the study area. We have not accounted for any possible temperature difference, but indications are that a thermal gradient sufficiently large to affect the relative strength did not exist (Wodicka et al., 2000; Marsh et al., 2009).

3.5. Sensitivity

The two largest uncertainties in the calculation of weakening across the transect are the viscosity contrast between panels and shear zones on Boomerang and Dogleg Islands and the viscosity contrast between panels on Matches and Boomerang and Dogleg Islands. In the analysis above, we suggest that the deformation in the panels within the Twelve Mile Bay shear zone core resulted from them being weaker than the panels on Matches. An unlikely alternative is that the panels are of comparable strength and that the higher bulk strains in the core caused higher strain in those panels. Although the petrological observation that hydration and amphibolite facies metamorphism went further towards completion approaching the Twelve Mile Bay shear zone supports our preferred interpretation, we cannot rule out the possibility that panels retained similar strengths throughout. In the other direction, panel weakening by much more than a factor of two would likely yield only a small viscosity contrast between the panels and the networked shear zones, contrary to the indications of the developed structures. Therefore, given that the panels exist into the Twelve Mile Bay shear zone and that the original lithologies were similar, we infer that deformed panels on Dogleg and Boomerang Islands are approximately a factor of two, and almost certainly not more than a factor of five, weaker than those on Matches Island.

We base our estimation of the viscosity contrast between panels and shear zones on Boomerang and Dogleg Islands on two measures: comparing relative shear strains in the panels and a qualitative visual observation of strain (Fig. 5). These measures are not well constrained, and we suggest that the viscosity contrast could reasonably be considered to lie between 2 and 10. This range affects our aggregate results by ~20% at our preferred strength contrast of two between Matches and Boomerang–Dogleg Island panels (Table 3).

Considering both significant uncertainties (Table 3), we suggest that a minimum weakening across the transect is 46%, for the case where the panels in all locations are the same strength. For a case of ten times weaker panels, coupled with a panel-shear zone viscosity contrast of ten, weakening could be as much as 97%, or nearly two orders of magnitude. We do not see either combination of factors as reasonable, however, given the geometrical and petrological observations. Our suggested weakening value, 77%, lies near the center of the range we considered (Table 3). Recalling that the analyzed sites are not within the core of the Twelve Mile Bay shear zone, we conclude that the Twelve Mile Bay shear zone core approached or exceeded an order of magnitude weakening relative to its protolith. Further support for the calculated strength drop lies in the first-order observation that the interior Parry Sound domain remained undeformed during the long transport along the Twelve Mile Bay shear zone.

Table 1
Bulk weakening with varying viscosity contrast at each study site.

Matches Island	UTM (NAD83) 17T			
19% shear zones by area	E567539 N4999439			
Panel-shear zone viscosity contrast	2	5	10	50
% weakening relative to panel strength	12%	23%	31%	48%
Dogleg Island	UTM (NAD83) 17T			
33% shear zones by area	E570140 N4995099			
Panel-shear zone viscosity contrast	2	5	10	50
% weakening relative to panel strength	23%	51%	68%	89%
Boomerang Island	UTM (NAD83) 17T			
43% shear zones by area	E568131 N4995980			
Panel-shear zone viscosity contrast	2	5	10	50
% weakening relative to panel strength	28%	56%	72%	91%

4. Discussion

4.1. Magnitude of bulk weakening along Parry Sound domain margin compared to other weakening processes

The weakening we document as a result of tectonism and metamorphism along the Twelve Mile Bay shear zone is greater than any of the processes, with the exception of melting, discussed in Section 2.2. We attribute this first to the fact that our calculations

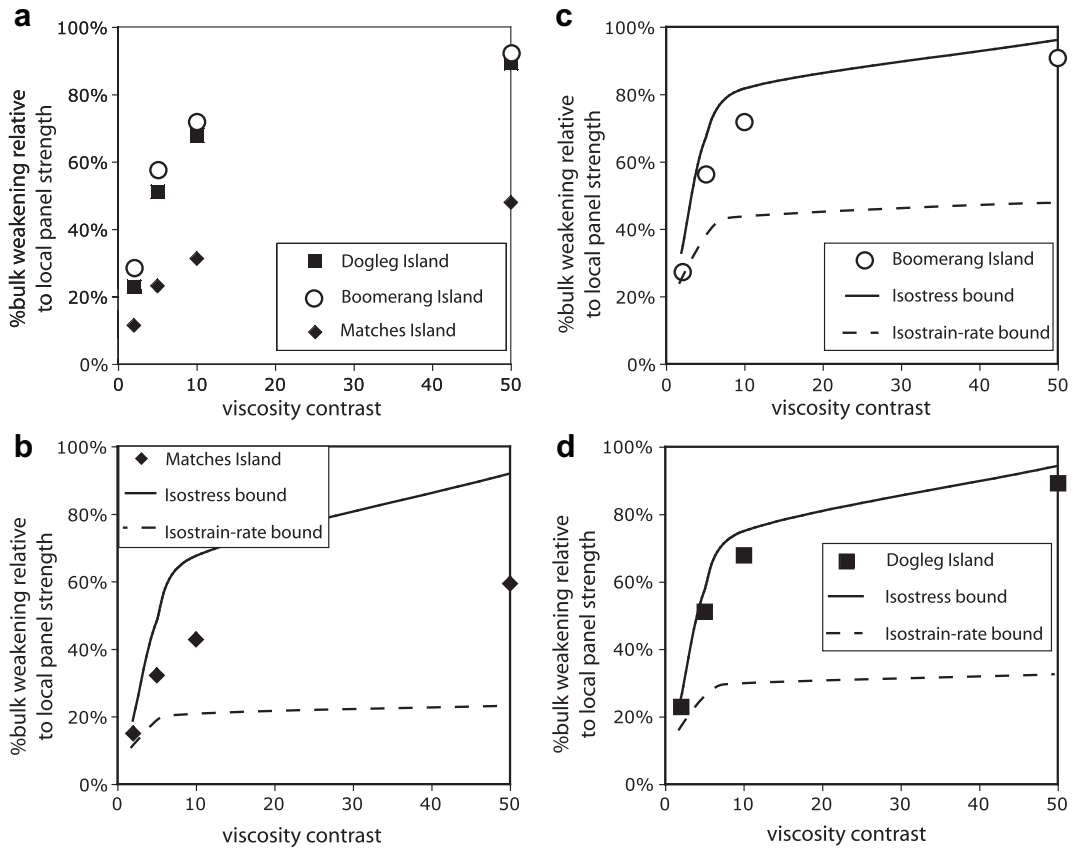

Fig. 8. (a) Degree of bulk weakening relative to local panel strength as a function of viscosity contrast between panels and shear zones for the three study sites. (b–d) Comparison of numerically calculated weakening with isostress and isostrain-rate bounds for each studied location.

apply to weakening across a single structure rather than the aggregate regional strength. In experiments, such as those by Holyoke and Tullis (2006), only bulk strength, combining the weak and strong components, is measurable. Second, the site we analyzed was a major crustal shear zone and therefore must have undergone significant weakening in order to develop. So our results are not surprising; rather, they demonstrate that strength changes due to hydration-induced metamorphic and textural changes can be substantial. Nevertheless, such weakening does not approach that possible due to melting.

We have considered strength changes over time, during the development of the Twelve Mile Bay shear zone, with the result being a spatial strength variation of approximately an order of magnitude. This scale of spatial variation is in good agreement with that of Houseman et al. (2008) and Treagus (1999). Houseman et al. (2008), who investigated several shear zones in the Sierra Nevada at centimeter, meter, and kilometer scales, suggested that an order of magnitude or slightly more is a reasonable upper limit for the effective viscosity contrasts there. Treagus (1999), based on her evaluation of cleavage refraction, suggested that effective viscosity variation between stratigraphic layers does not typically exceed an order of magnitude.

Throughout the viscous portion of the crust, in the absence of melt, temperature is usually considered as the largest control on strength. For typical flow laws (e.g., Hirth et al., 2001; Rybacki et al., 2006), a temperature change from 550 to 700 °C at a pressure of 0.8 GPa yields an effective viscosity change of 1–3 orders of magnitude. At the low end, the values are comparable to the results of this study. Considering that weakening due to textural and metamorphic changes does not require any long-distance mass or heat transfer to operate, it can rival or exceed the impact of temperature change at certain locations within an orogen. Away from the Twelve Mile Bay shear zone core, across a transect of at least 5 km, the degree of weakening diminishes towards the interior Parry Sound domain. We do not have sufficient measurements to describe that gradient, but given the analysis of Matches Island, which lies near the border of Twelve Mile Bay shear zone influence we infer the weakening to be greater than 30% across much of that distance.

Table 2
Proportional distance of numerically calculated strength drop[a] between isostress and isostrain-rate bounds[b].

	Viscosity contrast between panel and shear zone			
	2	5	10	50
Matches Is.	0.51	0.53	0.53	0.47
Dogleg Is.	0.22	0.19	0.15	0.08
Boomerang Is.	0.40	0.35	0.28	0.14

[a] Using the results shown in Table 1.
[b] A value of 1 represents the isostrain-rate bound; 0 represents the isostress bound.

4.2. Affect on crustal rheology

Many have long recognized the influence of strength variation on orogen development (e.g., Harry et al., 1995). Recent numerical studies have better quantified the impact of both temporal and spatial strength variation induced by structural, anatectic, and metamorphic processes (e.g., Beaumont et al., 2001; Culshaw et al., 2006; Jamieson et al., 2007; Groome et al., 2008). The effect is comparable to that of focused erosion driving advective mass transfer and accompanying thermal weakening (Zeitler et al., 2001; Koons et al., 2003; Barker, 2007), but occurs under different tectonic

Table 3
Bulk weakening on Boomerang and Dogleg Islands relative to panels on Matches Island for different viscosity contrasts.

		Panel-shear zone viscosity contrast on Dogleg and Boomerang Islands		
		2	5	10
Viscosity contrast between panels on Matches Island and those on Dogleg and Boomerang Islands	1	25%	54%	70%
	2	63%	77%	85%
	5	85%	91%	94%
	10	93%	95%	97%

conditions. Whereas the boundary conditions related to focused erosion are rooted in fairly well-constrained data, the magnitude of structural-metamorphic strength variation used in the models is somewhat more speculative. Nevertheless, orogen-scale numerical models representative of the region surrounding the Parry Sound domain (Jamieson et al., 2007) replicate the first-order geologic features of the Parry Sound region well by using a crust with initial lateral strength variation. In comparison, our results applied at the orogen scale would likely affect second-order features.

4.3. Comparison between numerical method and theoretical bounds

The results presented above rely on numerical calculations of bulk strength of a two-phase material. Comparing the results with the analytical solutions of the isostrain-rate and isostress bounds (Fig. 8, Table 2) demonstrates the importance of the phase arrangement and viscosity contrast in controlling bulk strength. For Matches Island, the proportional distance of our results between the theoretical bounds remains relatively constant with changing viscosity contrast. However, the proportional distance changes significantly for Dogleg and Boomerang Islands, approaching the isostress bound with greater viscosity contrast. A full analysis of the role of viscosity contrast and its importance relative to phase abundance and arrangement is beyond the scope of this paper. Nevertheless, these results imply that the position of true bulk strength relative to the isostrain-rate and isostress bounds can depend significantly on phase viscosity contrast.

5. Summary

The Twelve Mile Bay shear zone in southeastern Ontario accommodated many tens of kilometers of transport of the granulitic Parry Sound domain over underlying amphibolite facies domains between ca. 1160 and 1050 Ma, during an episode of Grenvillian orogenesis. The master shear zone formed in large part from Parry Sound domain rocks weakened by infiltrated fluid, metamorphism in the upper amphibolite facies, and interconnection of meter-scale shear zones. The core of the Twelve Mile Bay shear zone comprises nearly fully transposed gneiss, but outside the core numerous protolith relicts exist. Our numerical calculations, based on naturally occurring meter-scale shear zone geometries, indicate that the core of the Twelve Mile Bay shear zone is approximately an order of magnitude weaker than the rocks from which it formed. Moreover, weakening relative to the protolith is 30% or greater several kilometers from the shear zone core.

Acknowledgments

The University of Maine, NSF award EAR-0837922, and an NSERC Discovery Grant provided funding for the project. We thank Mark Jessell, Lynn Evans, and Greg Houseman for assistance in running the Basil calculations. Paul Bons and Lori Kennedy provided helpful reviews that allowed us to strengthen the manuscript, and we thank Cees Passchier for his editorial assistance.

References

Barker, A.D., 2007. 3D mechanical evolution of the plate boundary corner in SE Alaska. Unpublished M.S. thesis, University of Maine.
Barr, T.D., Houseman, G.A., 1996. Deformation fields around a fault embedded in a non-linear ductile medium. Geophysical Journal International 125, 473–490.
Beaumont, C., Jamieson, R.A., Nguyen, M.H., Lee, B., 2001. Himalayan tectonics explained by extrusion of a low-viscosity crustal channel coupled to focused surface denudation. Nature 414, 738–742.
Bons, P.D., Koehn, D., Jessell, M.W., 2008. Microdynamics Simulation. In: Lecture Notes in Earth Sciences. Springer.
Bons, P.D., Cox, S.J.D., 1994. Analogue experiments and numerical modelling on the relation between microgeometry and flow properties of polyphase materials. Materials Science and Engineering A A175, 237–245.
Brown, M., Solar, G.S., 2000. Feedback relations between deformation and melt, the evolution from weakening to hardening in transpressive orogens. Journal of the Czech Geological Society 45, 215–216.
Bürgmann, R., Dresen, G., 2008. Rheology of the lower crust and upper mantle: evidence from rock mechanics, geodesy, and field observations. Annual Review of Earth and Planetary Sciences 36, 531–567.
Bystricky, M., Heldelbach, F., Mackwell, S., 2006. Large-strain deformation and strain partitioning in polyphase rocks: dislocation creep of olivine–magnesio-wustite aggregates. Tectonophysics 427, 115–132.
Carreras, J., 2001. Zooming on northern Cap de Creus shear zones. Journal of Structural Geology 23, 1457–1486.
Cruden, A.R., 1990. Flow and fabric development during the diapiric rise of magma. Journal of Geology 98, 681–698.
Culshaw, N.G., Beaumont, C., Jamieson, R.A., 2006. The orogenic superstructure–infrastructure concept: revisited, quantified, and revived. Geology 34, 733–736.
Culshaw, N.G., Corrigan, D., Ketchum, J.W.F., Wallace, P., Wodicka, N., Easton, R.M., 2004. Georgian Bay geological synthesis, Grenville Province: explanatory notes for preliminary maps P.3548 to P.3552. In: Open File Report – Ontario Geological Survey, Report: 6143, p. 28.
Culshaw, N.G., Gerbi, C., 2009. Modes of flow in the orogenic infrastructure: the example of the Central Gneiss. Geological Society of America Abstracts with Programs 87, 41–43.
Culshaw, N.G., Jamieson, R.A., Ketchum, J.W.F., Wodicka, N., Corrigan, D., Reynolds, P.H., 1997. Transect across the northwestern Grenville orogen, Georgian Bay, Ontario: polystage convergence and extension in the lower orogenic crust. Tectonics 16, 966–982.
Dahlen, F.A., Suppe, J., Davis, D., 1984. Mechanics of fold-and-thrust belts and accretionary wedges: cohesive Coulomb theory. Journal of Geophysical Research 89, 10087–10101.
Davidson, A., 1984. Tectonic boundaries within the Grenville, Province of the Canadian shield. Journal of Geodynamics 1, 433–444.
Davidson, A., Culshaw, N.G., Nadeau, L., 1982. A tectono-metamorphic framework for part of the Grenville Province, Parry Sound region, Ontario. Current Research, Geological Survey of Canada 82-1A, 175–190.
Dell'Angelo, L.N., Tullis, J., 1996. Textural and mechanical evolution with progressive strain in experimentally deformed aplite. Tectonophysics 256, 57–82.
Dimanov, A., Dresen, G., 2005. Rheology of synthetic anorthite–diopside aggregates: implications for ductile shear zones. Journal of Geophysical Research – Solid Earth 110, B07203.
Evans, B., 2005. Creep constitutive laws for rocks with evolving structure. In: Geological Society Special Publications, vol. 245, pp. 329–346.
Groome, W.G., Johnson, S.E., Koons, P.O., 2006. The effects of porphyroblast growth on the effective viscosity of metapelitic rocks: implications for the strength of the middle crust. Journal of Metamorphic Geology 24, 389–407.
Groome, W.G., Koons, P.O., Johnson, S.E., 2008. Metamorphism, transient mid-crustal rheology, strain localization and the exhumation of high-grade metamorphic rocks. Tectonics 27, TC1001.
Handy, M.R., 1990. The solid-state flow of polymineralic rocks. Journal of Geophysical Research – Solid Earth and Planets 95, 8647–8661.
Handy, M.R., 1994. Flow Laws for rocks containing 2 nonlinear viscous phases – a phenomenological approach. Journal of Structural Geology 16, 287–301.
Handy, M.R., Brun, J.P., 2004. Seismicity, structure and strength of the continental lithosphere. Earth and Planetary Science Letters 223, 427–441.
Handy, M.R., Hirth, G., Bürgmann, R., 2007. Continental fault structure and rheology from the frictional-to-viscous transition downward. In: Handy, M.R., Hirth, G., Hovius, N. (Eds.), Tectonic Faults: Agents of Change on a Dynamic Earth. MIT Press, Cambridge, MA, pp. 139–181.
Handy, M.R., Wissing, S.B., Streit, L.E., 1999. Frictional–viscous flow in mylonite with varied bimineralic composition and its effect on lithospheric strength. Tectonophysics 303, 175–191.

Harry, D.L., Oldow, J.S., Sawyer, D.S., 1995. The growth of orogenic belts and the role of crustal heterogeneities in decollement tectonics. Geological Society of America Bulletin 107, 1411–1426.
Hirth, G., Teyssier, C., Dunlap, W.J., 2001. An evaluation of quartzite flow laws based on comparisons between experimentally and naturally deformed rocks. International Journal of Earth Sciences 90, 77–87.
Holl, A., Althaus, E., Lempp, C., Natau, O., 1997. The petrophysical behaviour of crustal rocks under the influence of fluids. Tectonophysics 275, 253–260.
Holyoke III, C.W., Tullis, J., 2006. Mechanisms of weak phase interconnection and the effects of phase strength contrast on fabric development. Journal of Structural Geology 28, 621–640.
Houseman, G., Barr, T., Evans, L., 2008. Basil: computation of stress and deformation in a viscous material. In: Bons, P.D., Koehn, D., Jessell, M.W. (Eds.), Microdynamics Simulation. Lecture Notes in Earth Sciences. Springer, Berlin, pp. 139–154.
Hueckel, T., Peano, A., Pellegrini, R., 1994. A thermo-plastic constitutive law for brittle–plastic behavior of rocks at high temperatures. Pure and Applied Geophysics 143, 483–511.
Jackson, J., 2002. Strength of the continental lithosphere: time to abandon the jelly sandwich? GSA Today 12, 4–10.
Jamieson, R.A., Beaumont, C., Nguyen, M.H., Culshaw, N.G., 2007. Synconvergent ductile flow in variable-strength continental crust: numerical models with application to the western Grenville orogen. Tectonics 26, TC5005.
Jessell, M.W., Siebert, E., Bons, P.D., Evans, L., Piazolo, S., 2005. A new type of numerical experiment on the spatial and temporal patterns of localization of deformation in a material with a coupling of grain size and rheology. Earth and Planetary Science Letters 239, 309–326.
Jessell, M.W., Bons, P.D., Griera, A., Evans, L., Wilson, C.J.L., 2009. A tale of two viscosities. Journal of Structural Geology 31, 719–736.
Ji, S., 2004. A generalized mixture rule for estimating the viscosity of solid–liquid suspensions and mechanical properties of polyphase rocks and composite materials. Journal of Geophysical Research 109, B10207.
Ji, S.C., Wang, Q., Xia, B., Marcotte, D., 2004. Mechanical properties of multiphase materials and rocks: a phenomenological approach using generalized means. Journal of Structural Geology 26, 1377–1390.
Johnson, S.E., Vernon, R.H., Upton, P., 2004. Foliation development and progressive strain-rate partitioning in the crystallizing carapace of a tonalite pluton: microstructural evidence and numerical modeling. Journal of Structural Geology 26, 1845–1865.
Jordan, P.G., 1987. The deformational behaviour of bimineralic limestone–halite aggregates. Tectonophysics 135, 185–197.
Kohlstedt, D.L., Evans, B., Mackwell, S.J., 1995. Strength of the lithosphere: constraints imposed by laboratory experiments. Journal of Geophysical Research 100, 17587–17602.
Koons, P.O., Norris, R.J., Craw, D., Cooper, A.F., 2003. Influence of exhumation on the structural evolution of transpressional plate boundaries: an example from the Southern Alps, New Zealand. Geology 31, 3–6.
Krogh, T.E., Kwok, Y.Y., 2005. The age enigma in the Moon River structure and the Parry Sound domain connection, Grenville Province. Geological Association of Canada Abstracts with Program 30, 106.
Larsen, C.F., Motyka, R.J., Freymueller, J.T., Echelmeyer, K.A., Ivins, E.R., 2005. Rapid viscoelastic uplift in Southeast Alaska caused by post-Little Ice Age glacial retreat. Earth and Planetary Science Letters 237, 548–560.
Lonka, H., Schulmann, K., Venera, Z., 1998. Ductile deformation of tonalite in the Suomusjarvi shear zone, south-western Finland. Journal of Structural Geology 20, 783–798.
Marsh, J.H., Gerbi, C.C., Culshaw, N.G., 2009. On the role of fluids in deep crustal shear zones. Geological Society of America Abstracts with Program 41 (3).
Montesi, L.G.J., Zuber, M.T., 2002. Parametric analysis of localization during a variety of geological conditions. Journal of Geophysical Research 107, B3. doi:10.1029/2001JB000465.
Park, Y., Yoo, S.-H., Ree, J.-H., 2006. Weakening of deforming granitic rocks with layer development at middle crust. Journal of Structural Geology 28, 919–928.
Pinkerton, H., Stevenson, R.J., 1992. Methods of determining the rheological properties of magmas at sub-liquidus temperatures. Journal of Volcanology and Geothermal Research 53, 47–66.
Ramsay, J.G., Huber, M.I., 1987. The techniques of modern structural geology. Strain analysis, vol. 1, Academic Press, London.
Reuss, A., 1929. Berechnung der Fliessgrenze von Mischkristallen auf Grund der Plastizitatsbedingung fur Einkristalle. Zeitschrift für Angewandte Mathematik und Mechanik 9, 49–58.
Rivers, T., 1997. Lithotectonic elements of the Grenville Province: review and tectonic implications. Precambrian Research 86, 117–154.
Rosenberg, C.L., Handy, M.R., 2005. Experimental deformation of partially melted granite revisited: implications for the continental crust. Journal of Metamorphic Geology 23, 19–28.
Ross, J.V., Wilks, K.R., 1996. Microstructure development in an experimentally sheared orthopyroxene granulite. Tectonophysics 256, 83–100.
Rubie, D.C., 1983. Reaction-enhanced ductility: the role of solid–solid univariant reactions in deformation of the crust and mantle. Tectonophysics 96, 331–352.
Rutter, E.H., 1999. On the relationship between the formation of shear zones and the form of the flow law for rocks undergoing dynamic recrystallization. Tectonophysics 303, 147–158.
Rybacki, E., Gottschalk, M., Wirth, R., Dresen, G., 2006. Influence of water fugacity and activation volume on the flow properties of fine-grained anorthite aggregates. Journal of Geophysical Research – Solid Earth 111, B03203.
Rybacki, E., Paterson, M.S., Wirth, R., Dresen, G., 2003. Rheology of calcite–quartz aggregates deformed to large strain in torsion. Journal of Geophysical Research – Solid Earth 108.
Takeda, Y.-T., Griera, A., 2006. Rheological and kinematical responses to flow of two-phase rocks. Tectonophysics 427, 95–113.
Treagus, S.H., 1999. Are viscosity ratios of rocks measurable from cleavage fraction? Journal of Structural Geology 21, 895–901.
Treagus, S.H., 2002. Modelling the bulk viscosity of two-phase mixtures in terms of clast shape. Journal of Structural Geology 24, 57–76.
Treagus, S.H., Lan, L., 2003. Simple shear of deformable square objects. Journal of Structural Geology 25, 1993–2003.
Treagus, S.H., Lan, L.B., 2004. Deformation of square objects and boudins. Journal of Structural Geology 26, 1361–1376.
Tullis, T.E., Horowitz, F.G., Tullis, J., 1991. Flow laws of polyphase aggregates from end-member flow laws. Journal of Geophysical Research – Solid Earth and Planets 96, 8081–8096.
Twiss, R.J., Moores, E.M., 1992. Structural Geology. W.H. Freeman, New York.
Upton, P., Craw, D., 2008. Modelling the role of graphite in development of a mineralised mid-crustal shear zone, Macraes Mine, New Zealand. Earth and Planetary Science Letters 266, 245–255.
van Breeman, O., Davidson, A., Loveridge, W.D., Sullivan, R.D., 1986. U–Pb Zircon Geochronology of Grenvillian Tectonites, Granulites and Igneous Precursors, Parry Sound, Ontario. The Grenville Province, Geological Association of Canada, Special Paper 31, pp. 191–207.
Voigt, W., 1928. Lehrbuch der Kristallphysik. Teubner, Leipzig, Germany.
Wintsch, R.P., Christoffersen, R., Kronenberg, A.K., 1995. Fluid–rock reaction weakening of fault zones. Journal of Geophysical Research 100, 13021–13032.
Wodicka, N., Ketchum, J.W.F., Jamieson, R.A., 2000. Grenvillian metamorphism of monocyclic rocks, Georgian Bay, Ontario, Canada: implications for convergence history. Canadian Mineralogist 38, 471–510.
Wu, P., Mazzotti, S., 2007. Effects of a lithospheric weak zone on postglacial seismotectonics in Eastern Canada and the Northeastern United States. Special Paper - Geological Society of America 425, 113–128.
Zeitler, P.K., Koons, P.O., Bishop, M.P., Chamberlain, C.P., Craw, D., Edwards, M.A., Hamidullah, S., Jan, M.Q., Khan, M.A., Khattak, M.U.K., Kidd, W.S.F., Mackie, R.L., Meltzer, A.S., Park, S.K., Pecher, A., Poage, M.A., Sarker, G., Schneider, D.A., Seeber, L., Shroder, J.F., 2001. Crustal reworking at Nanga Parbat, Pakistan: metamorphic consequences of thermal–mechanical coupling facilitated by erosion. Tectonics 20, 712–728.
Zoback, M.D., 2000. Strength of the San Andreas. Nature 405, 31–32.